Polyhedron 27 (2008) 3710–3716

Contents lists available at ScienceDirect

Polyhedron

journal homepage: www.elsevier.com/locate/poly

Coordination of a mesogenic Schiff-base with Mn^{II}, Co^{II}, Ni^{II}, Cu^{II} and Zn^{II}: Synthesis, spectral studies and crystal structures

Angad Kumar Singh [a], Sanyucta Kumari [a], T.N. Guru Row [b], Jai Prakash [b], K. Ravi Kumar [c], B. Sridhar [c], T.R. Rao [a,*]

[a] Department of Chemistry, Banaras Hindu University, Varanasi 221005, India
[b] Indian Institute of Science, Bangalore 560012, India
[c] Indian Institute of Chemical Technology, Tarnaka, Hyderabad 500 007, India

ARTICLE INFO

Article history:
Received 2 July 2008
Accepted 13 September 2008
Available online 7 November 2008

Keywords:
Mesogenic Schiff-base
Low-spin distorted square-pyramidal Ni^{II} complex
Crystal structures
Square-planar complexes of Co^{II} and Cu^{II}

ABSTRACT

A novel mesogenic (*nematic*) Schiff-base, *N,N*′-di-4-(4′-pentyloxybenzoate)salicylidene diaminoethane, H_2dpbsde (abbreviated as H_2L^5) was synthesized and its structure studied. The Schiff-base crystallizes in the non-centrosymmetric space group $Pna2_1$ with $Z = 4$, and the mesogenic isomorphous nickel and copper complexes, $[NiL^5]_2$ and $[CuL^5]$, in the centrosymmetric space group $P2_1/c$ with $Z = 4$. The $(L^5)^{2-}$ species coordinates to the metal ions through two phenolate oxygens and two azomethine nitrogens. Both the $[NiL^5]_2$ and $[CuL^5]$ complexes involve *cis*-MN_2O_2 planes; the former complex has a low-spin distorted square-pyramidal geometry with a Ni–Ni bonding of 3.337 Å and the latter, a square-planar geometry.

1. Introduction

Liquid crystals with transition-metal core groups, called metallomesogens, have attracted increasing attention because of the possibility of combining the physico-chemical properties of the metal (color, magnetism, polarizability, redox behaviour etc.) with those of the organic framework [1–8]. Thus, the synthesis and study of metallomesogens has been a very active area of research for more than 20 years and different approaches have been adopted in order to accommodate different metal centres [9,10]. A major distinction between metallomesogens and organic mesogens is the greater tendency in the former type to exhibit intermolecular dative coordination in the solid state [11]. The major part of the metallomesogens extensively studied includes those complexes derived from salicylaldimine Schiff-bases [12–14]. As a part of our systematic investigation [15–18] on structural and spectroscopic studies of 3d metal complexes of a series of mesogenic salicylaldimine Schiff-base derivatives, we report here the results of our investigation on the synthesis, spectroscopic studies and crystal structures of the mesogenic Schiff-base, *N,N*′-di-4-(4′-pentyloxybenzoate)salicylidene diaminoethane (H_2L^5), and the corresponding 3d metal complexes.

2. Experimental

2.1. Starting materials

All reagents were purchased from commercial sources and were used as received: 4-hydroxy benzoic acid, 1-bromopentane, 2,4-dihydroxybenzaldehyde, *N,N*′-dicyclohexylcarbodiimide (DCC), *N,N*-dimethylaminopyridine (DMAP) and 1,2-diaminoethane are from Sigma–Aldrich, USA; all metal acetates and KOH are from Merck. The solvents received were dried using standard methods [19] when required.

2.2. Instrumentation

The ^1H and ^{13}C NMR spectra were recorded on a JEOL AL-300 MHz FT-NMR multinuclear spectrometer. C, H and N contents were microanalyzed on an Elemental Vario EL III Carlo Erba 1108 analyzer. Infrared spectra were recorded on a JASCO FT/IR (model-5300) spectrophotometer in the 4000–400 cm^{-1} region. Electronic spectra of the complexes in chloroform solutions were recorded on a Shimadzu spectrophotometer, model Pharmaspec UV-1700. The mass spectra were recorded on JEOL SX-102 (EI/FAB) mass spectrometers. Magnetic susceptibility measurements were made at room temperature on a Cahn-Faraday balance.

2.3. X-ray crystallographic data collection and refinement of the structure

X-ray data for the compounds H_2L^5 [*jpl5*], $[NiL^5]_2$ [*jpni1*] and $[CuL^5]$ [*ac27*] were collected using a Bruker AXS SMART APEX

---

* Corresponding author. Tel.: +91 542 2307326; fax: +91 542 2368127.
E-mail address: drtrrao@gmail.com (T.R. Rao).

0277-5387/$ - see front matter © 2008 Elsevier Ltd. All rights reserved.
doi:10.1016/j.poly.2008.09.013

CCD diffractometer using graphite monochromated Mo Kα ($\lambda = 0.7107$ Å) radiation and the intensities were measured using the ω scan method. Preliminary lattice parameters and orientation matrices were obtained from four sets of frames. Unit cell dimensions were determined from the setting angles of 6903 reflections in the range $2.17° < \theta < 25.79°$. Integration and scaling of intensity data was accomplished using the SAINT program [20]. The structure was solved by direct methods using SHELXS97 [21] and refinement was carried out by full-matrix least-squares techniques using SHELXL97 [21]. Anisotropic displacement parameters were included for all non-hydrogen atoms. The side chain atoms were disordered and refined with site-occupation factors of 0.563(7) and 0.437(7). The geometries of the disordered atoms were refined with distance restraints. The displacement parameters of the disordered atoms were restrained with SIMU and DELU commands.

2.4. Synthesis and analyses

N,N′-Di-4-(4′-pentyloxybenzoate)salicylidene diaminoethane, **3** (Scheme 1), was synthesized from the precursor materials **1** and **2**, as reported earlier [15,16]. The [ML^5] (M = Mn, Co, Ni, Cu and Zn) complexes were prepared by refluxing solutions of the Schiff-base H_2L^5 and the corresponding metal acetate in a 1:1 molar ratio in dichloromethane/ethanol medium for ~2 h at 80 °C. The reaction mixture was left overnight in the flask, closed with a guard tube. The solid complex that separated out in each case was filtered under suction and washed repeatedly with cold ethanol and dried over fused $CaCl_2$ in a desiccator.

2.4.1. Synthesis of N,N′-di-4-(4′-pentyloxybenzoate)salicylidene diaminoethane, H_2L^5

N,N′-Di-4-(4′-pentyloxybenzoate)salicylidene diaminoethane, H_2L^5, was prepared by mixing together absolute ethanolic solutions of 4-pentyloxy-(4′-formyl-3′-hydroxy)benzoate (16.42 g, 50 mmol, in 100 mL) and 1,2-diaminoethane (1.9 mL, 25 mmol in 10 mL) and magnetically stirring for ~1 h in the presence of a few drops of acetic acid and leaving the resultant solution overnight in the reaction flask at room temperature. The micro-crystalline product was suction-filtered, thoroughly washed with cold ethanol, recrystallized from a solution of absolute ethanol/chloroform (v/v, 1/1) and dried at room temperature; yield: 12.76 g (75%) as a yellow solid; mp 230 °C. Calc. for $C_{40}H_{44}N_2O_8$ (680.31): C, 70.57; H, 6.51; N, 4.11. Found: C, 70.53; H, 6.53; N, 4.13%.

2.4.2. Synthesis of the Mn^{II} complex

Yield: 0.50 g (68%) as a brown coloured solid; mp 200 °C (decomposes). Calc. for $C_{40}H_{42}MnN_2O_8$ (733.71): C, 65.48; H, 5.77; N, 3.82; Mn, 7.49. Found: C, 65.50; H, 5.74; N, 3.80; Mn, 7.52%.

2.4.3. Co^{II} complex

Yield: 0.52 g (70%) as an olive green solid; mp 210 °C (decomposes). Calc. for $C_{40}H_{42}CoN_2O_8$ (737.70): C, 65.12; H, 5.74; N, 3.80; Co, 7.99. Found: C, 65.15; H, 5.72; N, 3.81; Co, 8.01%.

2.4.4. Ni^{II} complex

Yield: 0.58 g (79%) as a dark orange solid; mp 255 °C. Calc. for $C_{40}H_{42}N_2O_8Ni$ (737.46): C, 65.15; H, 5.74; N, 3.80; Ni, 7.96. Found: C, 65.27; H, 5.80; N, 3.85; Ni, 8.01%.

2.4.5. Cu^{II} complex

Yield 0.52 g (70%) as a violet solid; mp 260 °C. Calc. for $C_{40}H_{42}N_2O_8Cu$ (742.32): C, 64.72; H, 5.70; N, 3.77; Cu, 8.56. Found: C, 64.77; H, 5.72; N, 3.80; Cu, 8.53%.

2.4.6. Zn^{II} complex

Yield 0.48 g (65%) as a white solid; mp 140 °C. Calc. for $C_{40}H_{42}N_2O_8Zn$ (744.16): C, 64.56; H, 5.69; N, 3.76; Zn, 8.79. Found: C, 64.57; H, 5.71; N, 3.77; Zn, 8.78%.

3. Results and discussion

3.1. Physical properties and spectral investigation

The Schiff-base ligand H_2L^5 as well as the metal complexes are soluble in chloroform, dichloromethane, DMF and DMSO, but are

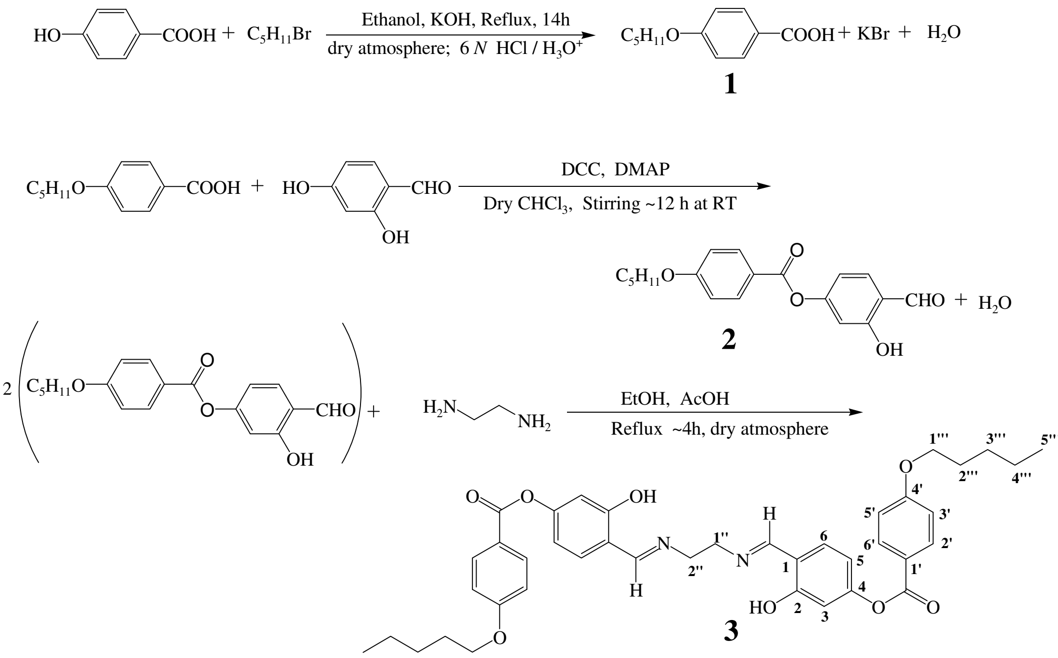

Scheme 1. Synthetic steps involved in the synthesis of **1** (*p*-pentyloxybenzoic acid), **2** (4-pentyloxy-(4′-formyl-3′-hydroxy)benzoate) and **3** (*N,N′*-di-4-(4′-pentyloxy benzoate)salicylidene diaminoethane, H_2L^5.

insoluble in water, methanol, ethanol and acetonitrile. The structure and purity of the parent ligand and the complexes were checked and confirmed by elemental analyses, IR, ^{1}H and ^{13}C NMR and FAB mass spectra. The mass spectral features of H_2L^5 were characterized by the base peak ($m/e = 191$ corresponding to the fragment $C_5H_{11}O$–Ph–CO^+), and the molecular ion peak ($m/e = 681$) with ∼72% intensity, and those of ML^5 (M = Mn^{II}, Co^{II}, Ni^{II} and Cu^{II}) by the base peak ($m/e = 121$ corresponding to the fragment, HO–Ph–CO^+) and the molecular ion peak ($m/e = 734$, 737, 737 and 742, respectively) with ∼92–98% intensity. Further, additional peaks (corresponding to the formation of dimeric units) were observed in the FAB mass spectra of the Mn^{II}, Co^{II} and Ni^{II} complexes; based on the decomposition behaviour of the former two complexes, they may be presumed to be polymeric, which upon bond rupture under the experimental conditions might give rise to dimeric units. A comparison of the ^{1}H and ^{13}C{^{1}H} NMR spectral data of the ligand with those of the diamagnetic Ni^{II} and Zn^{II} complexes shows the absence of the phenolic-OH signal (13.537 ppm) and a significant shift (8.358 to 7.195 and 8.458 ppm, respectively) in the peak position for –N═C*H* in the spectra of the metal complexes, which implies bonding through the phenolate anion and azomethine nitrogen atom [22] of the ligand. Similar shifts observed in the ^{13}C{^{1}H} NMR spectra were of considerable magnitude in the case of the carbon atoms directly attached to the bonding atoms. Thus, the NMR spectral data imply a tetra-dentate bonding of $(L^5)^{2-}$ through the two $\rangle$C═N groups and two phenolate oxygen atoms. In the IR spectrum of H_2L^5 the broad absorptions centred at 3443 cm^{-1} may be assigned to the ν(O–H)$_{\text{phenolic}}$ vibration, and further the strong bands occurring at 1740 and 1255 cm^{-1} may be assigned [23] to ν($\rangle$C═O) and ν(C–O) modes of the aromatic ester; the band occurring at 1628 cm^{-1} may be due to the ν(C═N) absorption of the azomethine moiety. These bands are shifted to lower frequencies in the complexes, indicating that the nitrogen atom of the azomethine group is coordinated to the metal ion [24]. Coordination through one of the nitrogen atoms of the ligand is also implied by the appearance of a new band (468–472 cm^{-1}) in the complexes, assignable to ν(M–N) [25,26]. Coordination through the phenolate oxygen to the metal ion is implied by the shifts of the ν(C–O) band in the complexes [27] and by the appearance of new bands, assignable to ν(M–O), in the 440–448 cm^{-1} region in the spectra of the complexes.

Table 2
Crystal structure data and structure refinement parameters

Details	Ligand, H_2L^5 [*jpl5*]	$[NiL^5]_2$ [*jpni1*]	$[CuL^5]$ [*ac27*]
Formula	$C_{40}H_{44}N_2O_8$	$C_{40}H_{42}N_2O_9Ni$	$C_{40}H_{43}N_2O_9Cu$
FW	680.77	737.47	759.30
Crystal system	Orthorhombic	Monoclinic	Monoclinic
Space group	*Pna*2$_1$	*P*2$_1$/*c*	*P*2$_1$/*c*
a (Å)	20.573(4)	17.8641(19)	17.7902(12)
b (Å)	5.868(1)	18.6864(19)	18.7711(13)
c (Å)	29.867(7)	11.4267(12)	11.4585(8)
β (°)	90	104.004(2)	104.355(1)
V (Å^3)	3605.8(13)	3701.0(7)	3707.0(4)
Z	4	4	4
ρ_{calc} (g/cm^3)	1.254	1.324	1.361
μ(Mo Kα) (mm^{-1})	0.087	0.579	0.647
R [$I > 2\sigma(I)$]	0.0637	0.0588	0.0449
R_w	0.1468	0.0924	0.0547
Goodness-of-fit	1.027	1.053	1.061
F(000)	1448	1552	1592
2θ Range (°)	1.98–25.00	1.17–25.00	1.18–25.00
Range of *h*, *k*, *l*	−24, 23	−21, 21	−21, 21
	−6, 6	−21, 22	−22, 22
	−35, 35	−13, 13	−13, 13
Total number of reflections	24264	26479	35252
Unique reflections	3228	6517	6537
Number of parameters	461	524	524
*wR*2_all	0.1680	0.1673	0.1419
*wR*2_obs	0.1296	0.1472	0.1299
$\Delta\rho_{\max}$, $\Delta\rho_{\min}$ (e Å^{-3})	0.296, −0.248	0.604, −0.485	0.723, −0.466

The room temperature magnetic moments and electronic spectral data of the present complexes are included in Table 1 while the spectra of the complexes of Co^{II}, Ni^{II} and Cu^{II} are shown in Fig. 1. The overall geometry assigned to the metal ion is based not only on the μ_{eff} values and the nature of the electronic spectra, but also

Table 1
Magnetic and electronic spectral data[a] of the complexes of H_2L5

Complex	Colour	μ_{eff} (B.M)	d–d transitions (nm)	Transition		Assignment
				Ground state(s)	Excited state(s)	
$[MnL^5]_n$	Brown	5.85	317, 260	$^6A_{1g}$	$^4A_{2g}$(F); ^4E_g(D)	Octahedral with M–M bonding
$[CoL^5]_n$	Olive green	3.52	974, 895, 860	^2E_g	$^2A_1$	Octahedral with M–M bonding (l.s.)
$[NiL^5]_2$	Dark orange	Diamag	530, 406	$^1A_1$	^1E; $^1A_2$	Square-pyramidal (M–M bonding[b] of 3.337 Å)
$[CuL^5]$	Violet	2.74	562	*xz*, *yz*	x^2–y^2	Sq. planar (M–M distance[b] of 3.457 Å)

[a] Spectra recorded in chloroform solutions.

[b] Vide single crystal structure data.

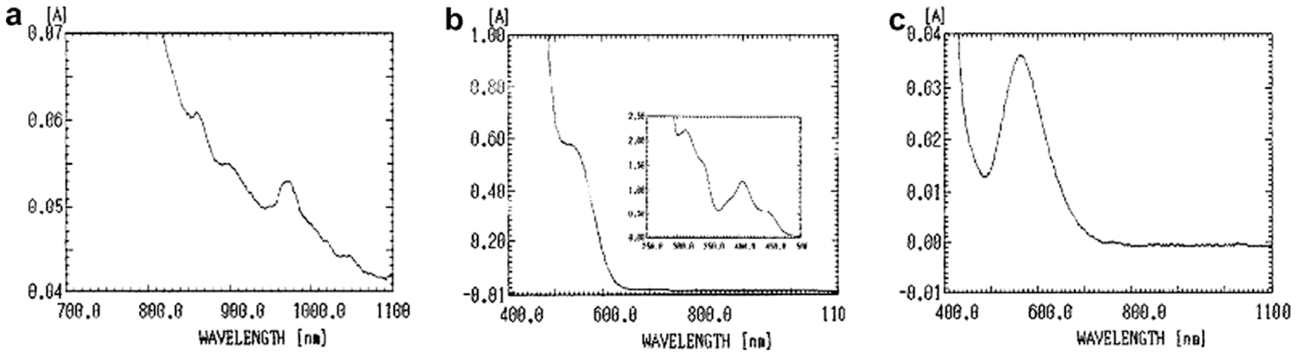

Fig. 1. Absorption spectra of: (**a**) $[CoL^5]$, (**b**) $[NiL^5]_2$ and (**c**) $[CuL^5]$.

on the denticity of the ligand (*vide* IR and NMR) and the number of such ligands coordinated to the metal ion (vide elemental analyses). Although the μ_{eff} values imply ferromagnetic type interactions in the Mn^{II}, Co^{II} and Cu^{II} complexes, no concrete conclusion to this effect could be drawn in the absence of variable temperature magnetic moment data. The $[MnL^5]_n$ complex gives rise to extremely weak bands in the electronic spectrum, presumably with an octahedral environment (square-planar units polymerically

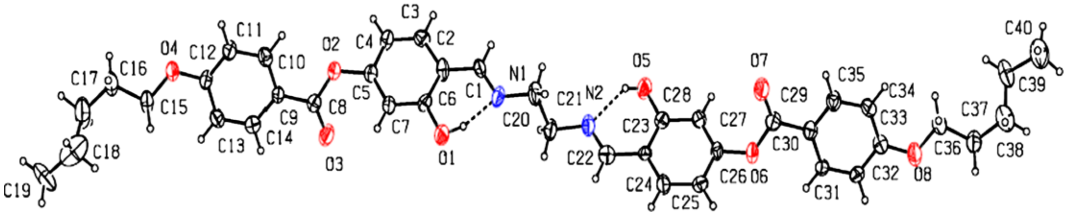

Fig. 2. The asymmetric unit of H_2L^5, with the atom numbering scheme. Displacement ellipsoids are drawn at the 30% probability level. H atoms are shown as small spheres of arbitrary radii. Hydrogen bonds are shown as dashed lines.

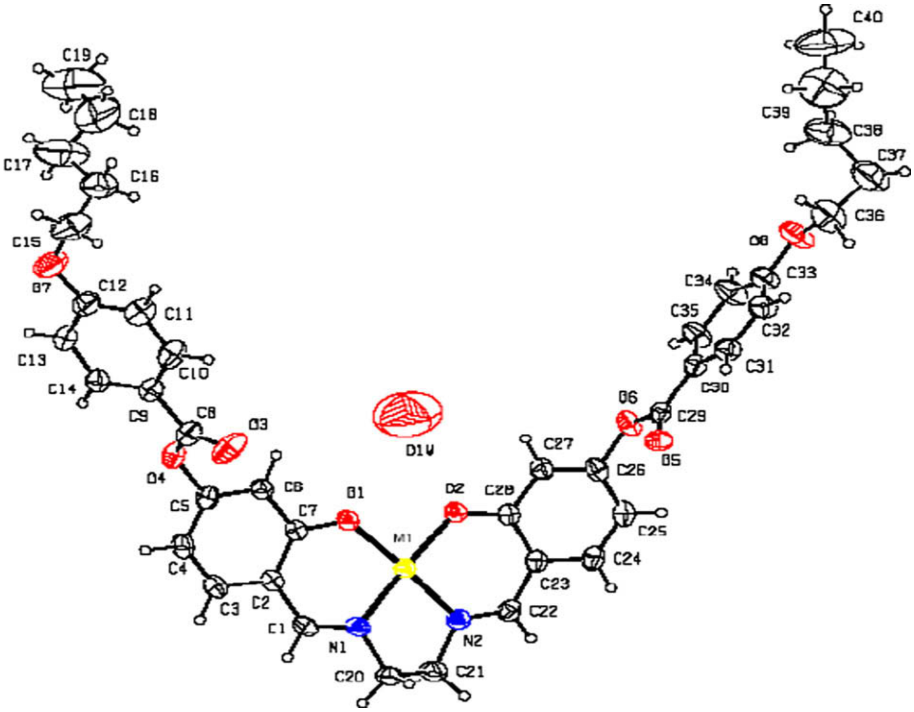

Fig. 3. The asymmetric unit of the isomorphous complexes $[ML^5]$ [M = Ni or Cu] with the atom numbering scheme. Displacement ellipsoids are drawn at the 30% probability level. The disordered atoms of the minor component (C161 and C361/C371/C381/C391/C401) have been omitted for clarity.

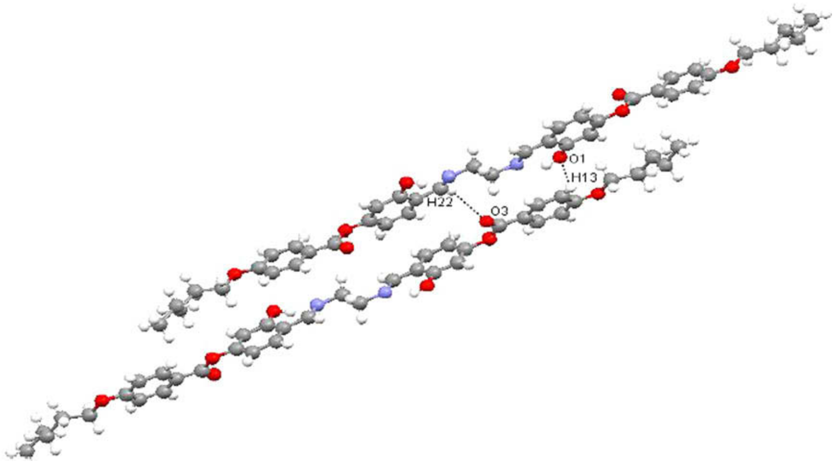

Fig. 4. A view of H_2L^5 molecules in the crystal lattice showing [C–H···O] intermolecular interactions along the *b* axis.

connected with M–M bonding) for the metal ion. The spectrum of the $[CoL^5]_n$ complex shows bands at 860, 895 and 974 nm which may be assigned to the transition(s) from the ^2E_g ground state to the $^2A_1$ excited state in an octahedral (low-spin) environment around the metal ion [28]. The electronic spectrum of the $[NiL^5]_2$ complex shows two absorptions at 406 and 530 nm which may be assigned to the ^1E and $^1A_2$ excited states from the $^1A_1$ ground state in a low-spin square-pyramidal environment of the diamagnetic metal ion [28]. The spectrum of $[CuL^5]$ shows a single band at 562 nm, assignable to the transition from the *xz*, *yz* ground state to the x^2–y^2 excited state in a square-planar environment [28].

3.2. Crystal structure and molecular association

The crystal data and structure refinement details for H_2L^5, $[NiL^5]_2$ and $[CuL^5]$ are given in Table 2. The molecular structure and atomic labelling scheme of the ligand and its nickel and copper complexes are as shown in Figs. 2 and 3, respectively, while their packing diagrams are shown in Figs. 5, 6 and 8.

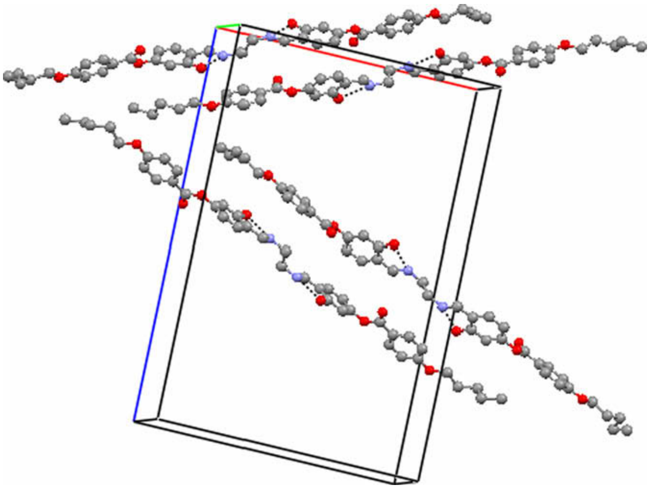

Fig. 5. Packing diagram of H_2L^5 showing intra molecular interactions along the *c* axis.

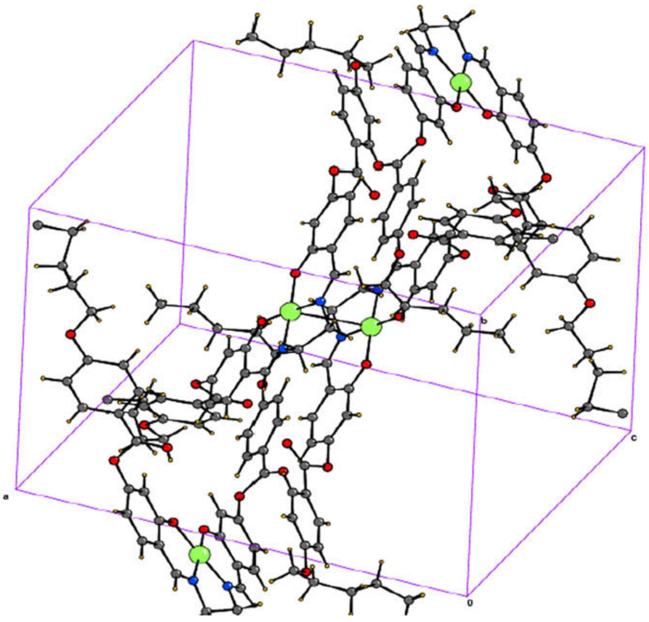

Fig. 6. Packing of molecules in the unit cell of $[NiL^5]_2$.

The Schiff-base crystallizes in the non-centrosymmetric space group *Pna*2_1 with *Z* = 4. The conformation of the ligand (Fig. 2) presents several interesting features: the molecule prefers to be as an extended linear conformation with all *trans* central linkages; the angle between the two six-membered rings adjacent to the central linkage is 0.39° (nearly planar); however, the angle between the adjacent rings in each flank is 52.50° (avg.); the extended arms of the aliphatic chains show large thermal vibrations compared to the central atoms, typical of any such molecule. Table 3 provides the details of the short intramolecular contacts while Fig. 4 represents a section of the intermolecular space, highlighting the C–H···O–H bond regions.

Both the isomorphic nickel and copper complexes $[NiL^5]_2$ and $[CuL^5]$ crystallize in the centrosymmetric space group *P*2_1/*c* with

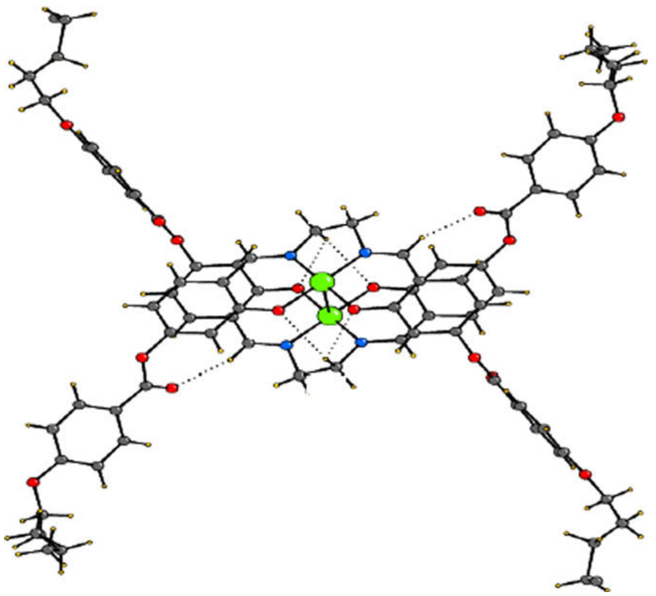

Fig. 7. A view of the $[NiL^5]_2$ molecule in the crystal lattice showing [C–H···O] inter molecular interactions.

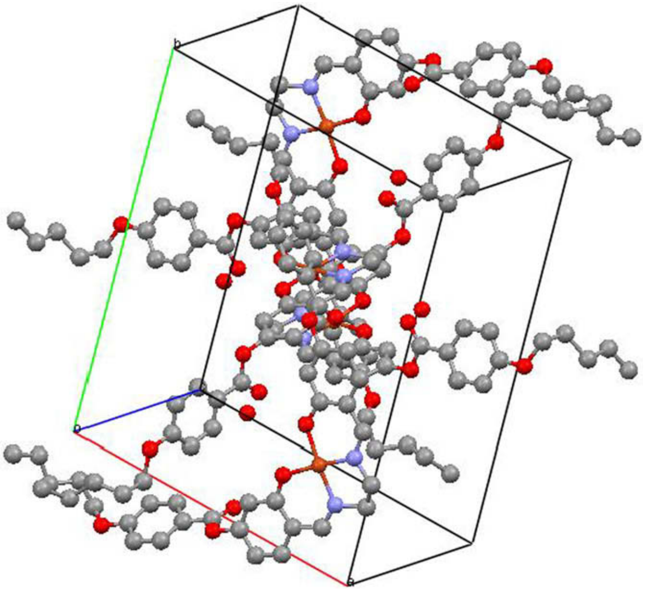

Fig. 8. Packing of molecules in the unit cell of $[CuL^5]$ along the *b* axis.

Table 3
Intramolecular hydrogen bonding data of H_2L^5

D–H···A	D–H (Å)	H···A (Å)	D···A (Å)	D–H···A (°)	Symmetry
O1–H1O...N1	0.87(7)	1.81(7)	2.582(10)	147(7)	*x*,*y*,*z*
O5–H5O...N2	0.86(9)	1.88(10)	2.576(10)	137(9)	*x*,*y*,*z*

Table 4
Selected bond lengths (Å) and bond angles (°) of the isomorphous $[NiL^5]_2$ and $[CuL^5]$[a] complexes

M1–O1	1.850(3) [1.8988(18)]	M1–N1	1.860(3) [1.933(2)]
M1–O2	1.848(3) [1.8956(17)]	M1–N2	1.846(4) [1.939(2)]
O1–M1–O2	84.9(1) [88.95(8)]	O1–M1–N2	178.0(2) [175.17(9)]
O1–M1–N1	94.6(2) [93.23(8)]	O2–M1–N2	94.7(1) [93.73(8)]
O2–M1–N1	177.2(2) [175.19(9)]	N2–M1–N1	85.9(2) [84.40(9)]

[a] The data for [CuL5] are given in square brackets.

Z = 4 and the ORTEP diagram is shown in Fig. 3. It appears that the ligand takes up an entirely different conformation, effectively generating a "V" shaped molecular unit. The coordination around Ni^{II} is believed to be a distorted square-pyramidal environment, generating a tricyclic moiety, while that around Cu^{II} is considered to be square-planar with a *cis*-conformation, which may be invoked on the basis of the four adjacent bond angles around the metal ion which are close to 90° (84.40(9), 88.95(8), 93.23(8), 93.73(8)) and the angles between the diagonal atoms of the square plane are close to 180° (175.19(9), 175.17(9)).

Table 4 describes the conformational features of the isomorphous Ni^{II} and Cu^{II} complexes. The angle between the two six-membered rings nearest to Ni is 2.92° while such an angle on the outside flanks is 73.81°. As expected, the thermal ellipsoids are once again large on the terminal chain atoms on either side. It is noteworthy that the conformations of the two flanks are different from each other, with one of the flanks displaying an intramolecular C–H···O interaction (C10–H10···O3). Also, the angle between the adjacent six-membered rings in one flank is 88.04° while in the other it is 56.82°. The angle between the planes containing the C24, O2, Ni1 and N2 atoms and C5, O1, Ni1 and N1 atoms is 2.74°. The Ni atom is penta-coordinated with a Ni–Ni metal bond of 3.336 Å; the distortion of the square base from planarity is quite negligible since the angles between the diagonal atoms of the square base are close to 180° (N2NiO1: 177.83 and N1NiO2: 177.17) in both the planes of the dimeric unit. Fig. 7 shows the packing features of $[NiL^5]_2$ along with the intermolecular interactions.

Table 5
Transition temperatures and enthalpy changes of H_2L^5 and of the $[NiL^5]_2$ and $[CuL^5]$ complexes

Compound	Transition[a]	T[b] (°C)	δH[b] (kJ mol^{-1})
H_2L^5	Cr–N	174.81	35.06
	N–I	229.30	10.81
	I–N	216.04	1.69
$[NiL^5]_2$	Cr–Cr	144.72	8.79
	Cr–N	245.09	19.52
	N–I[c] (dec.)	255.00	
$[CuL^5]$	Cr–Cr	136.21	10.07
	Cr–N	224.94	20.25
	N–I[c]	260.50	
	N–Cr	199.84	5.39

[a] Cr: Crystal, N: Nematic, I: Isotropic liquid.
[b] Data as obtained from the first DSC cycle.

The mesogenic nature of the ligand (H_2L^5) as well as the $[NiL^5]_2$ and $[CuL^5]$ complexes has been studied by two methods, using polarized optical microscopy and differential scanning calorimetry (DSC); the introduction of the metal ion into the metal-coordination sphere, as expected, resulted in the elevation of the transition temperature, melting and clearing points. The assignment of the mesophase (*nematic*) in each case is on the basis of the optical textures (Fig. 9a–c) and the DSC thermograms (Fig. 10a–c). The details of the transition temperatures, enthalpy changes and the mesophases of H_2L^5, $[NiL^5]$ and $[CuL^5]$ are given in Table 5. However, no such mesogenic property was observed with the complexes of Mn^{II}, Co^{II} and Zn^{II}.

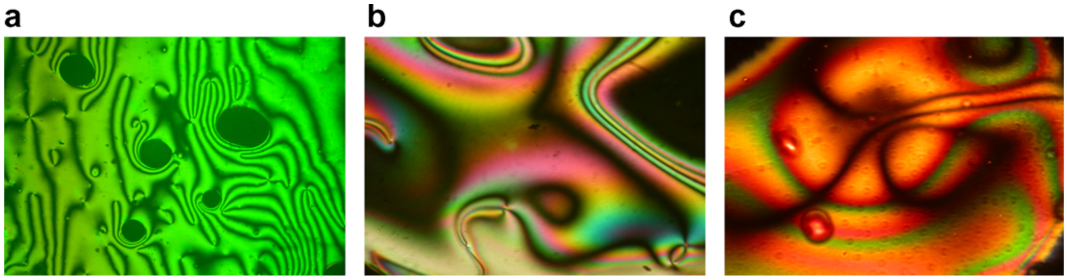

Fig. 9. Optical textures of: (a) H_2L^5 at 210 °C (b) $[NiL^5]_2$ at 252 °C and (c) $[CuL^5]$ at 245 °C.

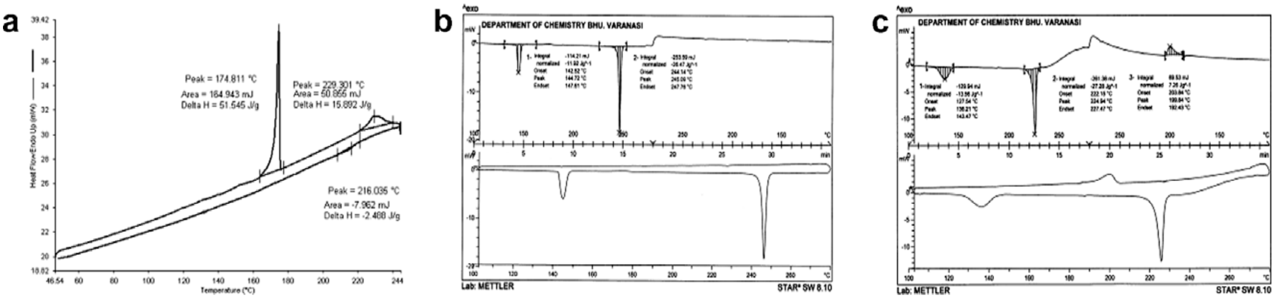

Fig. 10. DSC thermograms of: (**a**) H_2L^5 (**b**) $[NiL^5]_2$ and (**c**) $[CuL^5]$.

4. Conclusion

The mesogenic (*nematic)* Schiff-base *N,N*′-di-(4′-pentyloxybenzoate)salicylidene diaminoethane (H_2L^5) coordinates to Mn^{II}, Co^{II}, Ni^{II}, Cu^{II} and Zn^{II} to yield the isomorphous mesogenic (*nematic*) Ni^{II}, Cu^{II} complexes and the non-mesogenic Mn^{II}, Co^{II}, Zn^{II} complexes. The Schiff-base crystallizes in the non-centrosymmetric space group $Pna2_1$ with $Z = 4$ and the nickel and copper complexes, $[NiL^5]_2$ and $[CuL^5]$, in the centrosymmetric space group $P2_1/c$, with $Z = 4$. The coordination geometry around Ni^{II} is low-spin distorted square-pyramidal (*cis*-NiN_2O_2) while that of the Cu^{II} complex is square-planar with a *cis*-CuN_2O_2 configuration.

Acknowledgements

We wish to acknowledge the recording of FAB mass spectra and elemental analyses at the Central Drug Research Institute, Lucknow, India. One of the authors, T.R. Rao, gratefully acknowledges the financial grant received from the Council of Scientific & Industrial Research, New Delhi [vide Grant No. 01(1834)/03/EMR-II], the University Grants Commission, New Delhi [vide grant No. F.12-26/2003 (SR)] and the Department of Science and Technology, New Delhi [vide Grant No. SR/S1/IC-26/2004].

Appendix A. Supplementary data

CDC 660036, 660037 and 685718 contain the supplementary crystallographic data for this paper. These data can be obtained free of charge via http://www.ccdc.cam.ac.uk/conts/retrieving.html, or from the Cambridge Crystallographic Data Centre, 12 Union Road, Cambridge CB2 1EZ, UK; fax: (+44) 1223-336-033; or e-mail: deposit@ccdc.cam.ac.uk. Supplementary data associated with this article can be found, in the online version, at doi:10.1016/j.poly.2008.09.013.

References

[1] B. Donnio, D.W. Bruce, in: D.M.P. Mingos (Ed.), Structure and Bonding, Liquid Crystals II. Metallomesogens, Springer, 1999, p. 95.
[2] B. Donnio, D. Guillon, R. Deschenaux, D.W. Bruce, in: J.A. McCleverty, T.J. Meyer (Eds.), Metallomesogens in Comprehensive Coordination Chemistry, vol. 6, Elsevier, Oxford, 2003.
[3] A-M. Giroud-Godquin, P.M. Maitlis, Angew. Chem., Int. Ed. Engl. 30 (1991) 375.
[4] M.H. Chisholm, Acc. Chem. Res. 33 (2000) 53.
[5] P. Kirsch, M. Bremer, Angew. Chem., Int. Ed. Engl. 39 (2000) 4216.
[6] I. Aiello, M. Ghedini, M. La Deda, D. Pucci, O. Francescangeli, Eur. J. Inorg. Chem. (1999) 1367.
[7] J.L. Serrano, Metallomesogens: Synthesis, Properties and Applications, VCH, Weinheim, 1996.
[8] B. Donnio, D. Guillon, R. Deschenaux, D.W. Bruce, in: J.A. McCleverty, J.J. Meyer, M. Fujita, A. Powell (Eds.), Comprehensive Coordination Chemistry II, vol. 7, Elsevier, Oxford, 2003. p. 353.
[9] D.W. Bruce, R. Deschenaux, B. Donnio, D. Guillon, in: R.H. Crabtree, D.M.P. Mingos (Eds.), Comprehensive Organometallic Chemistry II, vol. 12, Elsevier, Oxford, UK, 2006, p. 195. Chapter 12.05.
[10] B. Donnio, D. Guillon, R. Deschenaux, D.W. Bruce, in: J.A. McCleverty, T.J. Meyer (Eds.), Comprehensive Coordination Chemistry, vol. 7, Elsevier, Oxford, UK, 2003, p. 357. Chapter 7.9.
[11] (a) A. Serrette, P.J. Carroll, T.M. Swager, J. Am. Chem. Soc. 114 (1992) 1887;
(b) A.M. Giroud-Godquin, P.M. Maitlis, Angew. Chem., Int. Ed. Engl. 30 (1991) 375.
[12] N. Hoshino, Coord. Chem. Rev. 174 (1998) 77.
[13] R. Paschke, D. Balkow, E. Sinn, Inorg. Chem. 41 (2002) 1949.
[14] (a) Y. Abe, K. Nakabayashi, N. Matsukawa, M. Iida, T. Tanase, M. Sugibayashia, K. Ohta, Inorg. Chem. Commun. 7 (2004) 580;
(b) Y. Abe, K. Nakabayashi, N. Matsukawa, H. Takashima, M. Iida, T. Tanase, M. Sugibayashi, H. Mukai, K. Ohta, Inorg. Chim. Acta 359 (2006) 3934;
(c) Y. Abe, N. Nakazima, T. Tanase, S. Katano, H. Mukai, K. Ohta, Mol. Cryst. Liq. Cryst. 466 (2007) 129;
(d) Y. Abe, A. Iyoda, K. Seto, A. Moriguchi, T. Tanase, H. Yokoyama, Eur. J. Inorg. Chem. 13 (2008) 2148.
[15] A.K. Singh, S. Kumari, K. Ravi Kumar, B. Sridhar, T.R. Rao, Polyhedron 27 (2008) 181.
[16] A.K. Singh, S. Kumari, K. Ravi Kumar, B. Sridhar, T.R. Rao, Polyhedron 27 (2008) 1937.
[17] N.V.S. Rao, M.K. Paul, T.R. Rao, A. Prasad, Liq. Cryst. 29 (2002) 1243.
[18] T.R. Rao, A. Prasad, Synth. React. Inorg. Met-Org. Nano-Metal Chem. 35 (2005) 299.
[19] A. Weisberger, F.S. Praskver, Organic Solvents, International Publishers Inc., New York, 1956. p. 1263.
[20] SMART and SAINT. Software Reference manuals. Versions 6.28a and 5.625, Bruker Analytical X-ray Systems Inc., Madison, Wisconsin, USA, 2001.
[21] G.M. Sheldrick, SHELXS97 and SHELXL97, Programs for crystal structure solution and refinement, University of Gottingen, Germany, 1997.
[22] K. Binnemans, K. Lodewyckx, R. van Deun, Y.G. Galyametdinov, D. Hinz, G. Meyer, Liq. Cryst. 28 (2001) 279.
[23] R.M. Silverstein, F.X. Webster, Spectroscopic Identification of Organic Compounds, 6th ed., John-Wiley & Sons. Inc., New York, 2002. pp. 82.
[24] A. Braibanti, F. Dallavalle, M.A. Pellinghelli, Inorg. Chem. 7 (1968) 1430.
[25] S.K. Agrawal, D.R. Tuflani, R. Gupta, S.K. Hajela, Inorg. Chim. Acta 129 (1987) 257.
[26] N. Saha, S. Sinha, Ind. J. Chem. 29 (1990) 292.
[27] K. Nakamoto, Infrared and Raman Spectra of Inorganic and Coordination Compounds, Wiley, New York, 1978.
[28] A.B.P. Lever, Inorganic Electronic Spectroscopy, Elsevier, Amsterdam, 1984. p. 490, 524, 571.